Modulating cell state to enhance suspension expansion of human pluripotent stem cells

Yonatan Y. Lipsitz[a], Curtis Woodford[a], Ting Yin[a], Jacob H. Hanna[b], and Peter W. Zandstra[a,c,d,e,f,1]

[a]Institute of Biomaterials and Biomedical Engineering, University of Toronto, Toronto, ON M5S 3G9, Canada; [b]Department of Molecular Genetics, Weizmann Institute for Science, Rehovot 76100, Israel; [c]CCRM, Toronto, ON M5G 1M1, Canada; [d]The Donnelly Centre for Cellular and Biomolecular Research, University of Toronto, Toronto, ON M5S 3E1, Canada; [e]Medicine by Design: A Canada First Research Excellence Fund Program, University of Toronto, Toronto, ON M5G 1M1, Canada; and [f]School of Biomedical Engineering, University of British Columbia, Vancouver, BC V6T 1Z3, Canada

Edited by Sang Yup Lee, Korea Advanced Institute of Science and Technology, Daejeon, Republic of Korea, and approved May 9, 2018 (received for review August 9, 2017)

The development of cell-based therapies to replace missing or damaged tissues within the body or generate cells with a unique biological activity requires a reliable and accessible source of cells. Human pluripotent stem cells (hPSC) have emerged as a strong candidate cell source capable of extended propagation in vitro and differentiation to clinically relevant cell types. However, the application of hPSC in cell-based therapies requires overcoming yield limitations in large-scale hPSC manufacturing. We explored methods to convert hPSC to alternative states of pluripotency with advantageous bioprocessing properties, identifying a suspension-based small-molecule and cytokine combination that supports increased single-cell survival efficiency, faster growth rates, higher densities, and greater expansion than control hPSC cultures. ERK inhibition was found to be essential for conversion to this altered state, but once converted, ERK inhibition led to a loss of pluripotent phenotype in suspension. The resulting suspension medium formulation enabled hPSC suspension yields 5.7 ± 0.2-fold greater than conventional hPSC in 6 d, for at least five passages. Treated cells remained pluripotent, karyotypically normal, and capable of differentiating into all germ layers. Treated cells could also be integrated into directed differentiated strategies as demonstrated by the generation of pancreatic progenitors (NKX6.1+/PDX1+ cells). Enhanced suspension-yield hPSC displayed higher oxidative metabolism and altered expression of adhesion-related genes. The enhanced bioprocess properties of this alternative pluripotent state provide a strategy to overcome cell manufacturing limitations of hPSC.

manufacturing | human pluripotent stem cells | cell state | suspension culture

Pluripotent stem cells (PSC) offer the opportunity to investigate fundamental questions in developmental biology and to advance the development of cell-based therapies (1). Human (h) PSC can be expanded indefinitely in culture while maintaining the ability to differentiate to all specialized cell types in a manner that parallels aspects of human development. These qualities render hPSC a particularly promising cell source for developing cell-based therapies to cure a variety of chronic conditions. However, a critical factor that currently limits the successful clinical translation of these therapies is the lack of robust, scalable technologies for manufacturing the quantities of cells anticipated to be required for widespread patient access (1, 2). For example, it is estimated that allogeneic cardiomyocyte replacement therapy for millions of Americans with heart disease would require 10^9 hPSC-derived cardiomyocytes per treatment (2). Generating this number of cardiomyocytes from traditional hPSC cultures may require large-scale differentiation processes preceded by a seed train of progressively larger hPSC expansion bioreactors. Drug screening using hPSC also requires efficient production of large quantities of hPSC-derived cells to screen drug libraries. While it has been widely demonstrated that mouse (m) PSC are capable of robust expansion in scalable suspension bioreactors commonly used in industrial manufacturing processes, with greater than 10-fold expansion in 4 d (3–11), attempts to expand hPSC in these systems have been plagued by low maximum cell densities and low yields (<3.5×10^6 cells/mL final cell density and <threefold equivalent expansion in 4 d) (12–17).

Our limited understanding of how cell states influence biomanufacturing outcomes restricts the strategies at our disposal for resolving these technology gaps. As our understanding of the molecular basis of pluripotency deepens, there is mounting evidence suggesting that PSC exist in multiple states of pluripotency that can be manipulated by genetic engineering or by changing culture conditions (18). In vitro, mPSC exist in distinct states exhibiting unique epigenetic characteristics, self-renewal signal requirements, and differentiation potentials. Two of these states share similarities with stages of embryonic development: the "naive" state resembles the preimplantation inner cell mass and the primed state resembles the later, postimplantation epiblast, which is "primed" toward differentiation (19, 20). The gene expression profile, epigenetic state, and signaling requirements of conventional hPSC resemble primed mPSC (18). Notably, mPSC have been cultured in conditions supporting the naive state in all high-yield, proof-of-principle bioreactor expansion experiments to date, while all hPSC bioreactor expansion studies to date have cultured cells in conditions supporting the conventional primed state. Motivated by the potential existence of multiple hPSC states, we hypothesized that cell-state differences, rather than species differences, could account for the low yields of hPSC cultured in suspension bioreactors relative to mPSC. Our efforts to generate an alternative, high-suspension-yield hPSC state

Significance

Efficient manufacturing is critical for the translation of cell-based therapies to clinical applications. To date, high-yield expansion of human pluripotent stem cells (hPSC) in suspension bioreactors has not been reported. Here, we present a strategy to shift suspension-grown hPSC to a high-yield state without compromising their ability to differentiate to all three germ layers. In this new state, hPSC expand to densities 5.7 ± 0.2-fold higher than conventional hPSC each passage in suspension bioreactors. High-density suspension cultures enable process intensification, cost reduction, and more efficient manufacturing. This work advances cell-state engineering as a valuable tool to overcome current challenges in therapeutic cell production and processing.

Author contributions: Y.Y.L. and P.W.Z. designed research; Y.Y.L., C.W., and T.Y. performed research; J.H.H. contributed new reagents/analytic tools; Y.Y.L. analyzed data; and Y.Y.L. wrote the paper.

Conflict of interest statement: J.H.H. is an advisor to Accelta Ltd. and Biological Industries Ltd.

This article is a PNAS Direct Submission.

This open access article is distributed under Creative Commons Attribution-NonCommercial-NoDerivatives License 4.0 (CC BY-NC-ND).

[1]To whom correspondence should be addressed. Email: peter.zandstra@utoronto.ca.

This article contains supporting information online at www.pnas.org/lookup/suppl/doi:10.1073/pnas.1714099115/-/DCSupplemental.

Published online June 4, 2018.

Downloaded at Palestinian Territory, occupied on December 4, 2021

ENGINEERING

APPLIED BIOLOGICAL SCIENCES

www.manaraa.com

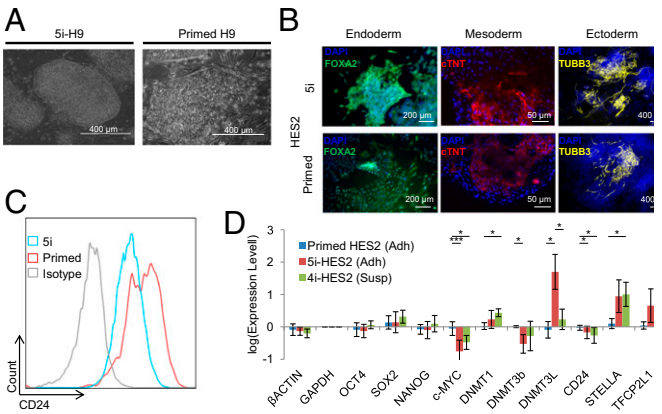

Fig. 1. A five inhibitor medium alters the morphology and gene expression of primed hPSC without impairing pluripotency. (*A*) Characteristic morphology of 5i-hPSC colonies consist of rounded smooth borders and tightly packed cells. Primed hPSC colonies consist of less densely packed cells and do not display smooth rounded borders. (*B*) 5i-hPSC are functionally pluripotent maintaining the capacity to differentiate to cells of all three germ layers. (*C*) 5i-hPSC have reduced expression of the CD24 surface marker used to track naive-state hPSC. (*D*) Expression levels of pluripotency-related factors in adherent primed hPSC, adherent 5i-hPSC, and suspension 4i-hPSC normalized to the average primed HES2 GAPDH level. Significant differences exist between both adherent 5i- and suspension 4i-HES2 and primed conditions. (Tukey's test: *, **, and *** indicate $P < 0.05$, 0.01, and 0.001, respectively. Biological replicates: primed $n = 4$, 5i-adherent $n = 9$, 4i-suspension $n = 6$. Error bars represent the SD.)

were guided by recent reports on the generation of naive state hPSC (21–27) which may have properties that are advantageous for manufacturing in suspension, including higher adherent single-cell survival efficiencies and accelerated adherent growth rates.

Here, we describe conditions which enable the conversion of conventional, primed hPSC to an alternative functional state characterized by significantly enhanced suspension expansion capabilities. We further demonstrate that using a well-characterized protocol, these 4i-hPSC can be directed to differentiate to pancreatic progenitors. These findings lay the groundwork for adopting cell-state conversion as a strategy to overcome current challenges in manufacturing hPSC and their derivatives for targeted cell therapy applications.

Results

hPSC Treated with 5i Have Altered Colony Morphology, Transcription Factor Expression, and Surface Marker Expression. Attempts to alter primed hPSC to resemble naive mPSC, known to exist in a stable state free from exogenous signaling (28), have incorporated various combinations of small-molecule inhibitors and genetic manipulation. We tested a protocol that has been reported to maintain naive hPSC with enhanced bioprocessing attributes in a mixture containing five inhibitors (5i), including PKC inhibition and p38 inhibition via the BIRB796 molecule (27). After treating H9 and HES2 hPSC with 5i, we observed the appearance of colonies with a raised morphology (Fig. 1*A*) that maintained high levels of expression of key pluripotency factors OCT4 and SOX2 for >15 passages (*SI Appendix*, Fig. S1). These stable "5i-hPSC" demonstrated functional pluripotency by maintaining the capacity to differentiate into cell types of all three germ layers (Fig. 1*B*). Consistent with our previously published findings (29), we observed reduced gene and protein expression of the surface marker CD24 in 5i-hPSC compared with primed hPSC (Fig. 1 *C* and *D*). In line with published reports on naive hPSC conversion (22, 23, 27), transcription factors *DNMT1*, *DNMT3L*, and *STELLA* were up-regulated, while *c-MYC* and *DNMT3B* were down-regulated in 5i-hPSC. We observed that changes in gene expression levels for core pluripotency factors *OCT4*, *SOX2*, and *NANOG* were negligible after transitioning primed hPSC to 5i-hPSC (Fig. 1*D*), demonstrating that these conditions maintain a core pluripotency gene regulatory network.

hPSC Treated with 5i Have Enhanced Bioprocessing Properties That Facilitate Increased Yields in Suspension Culture. We next characterized 5i-HPSC growth kinetics, ability to form aggregates in static suspension, and agitated suspension survival and expansion. In preparation for suspension expansion, the growth rates of feeder-based adherent 5i-hPSC was calculated. Higher proliferation rates were exhibited in 5i-hPSC relative to primed hPSC (Fig. 2*A*), leading to twice as many cells in 5i-hPSC cultures at day 6 post-seeding. Colonies formed from 5i-hPSC treatment were observed to be rounded at confluence, and a plateau stationary phase of growth was not clearly observed. Both 5i-H9 and 5i-HES2 had significantly lower exponential phase doubling times (21.1 ± 3.6 and 23.3 ± 0.7 h) than untreated hPSC (30.3 ± 4.7 and 31.2 ± 1.3 h) (*SI Appendix*, Fig. S2*A*).

Next, in static suspension conditions, we compared aggregate formation characteristics of 5i-hPSC to primed hPSC. Seeded as single cells at low density (100 cells per well in 96-well plate), suspension aggregate formation efficiencies were significantly higher in 5i-hPSC than in primed hPSC (4 ± 1 and 6 ± 1 fold higher using the HES2 and H9 cell lines, respectively) (Fig. 2*B*). This transition to suspension culture results in a feeder-free culture system. Eliminating the feeder layer, in addition to transitioning to the 5i medium composition which contains almost completely defined components (contains purified albumin), should reduce variability between manufacturing runs.

To evaluate 5i-hPSC survival and expansion as aggregates under dynamic suspension conditions, primed and 5i-hPSC were plated as single cells in low-attachment plates that were then placed on orbital shakers or into a small-scale bioreactor. After

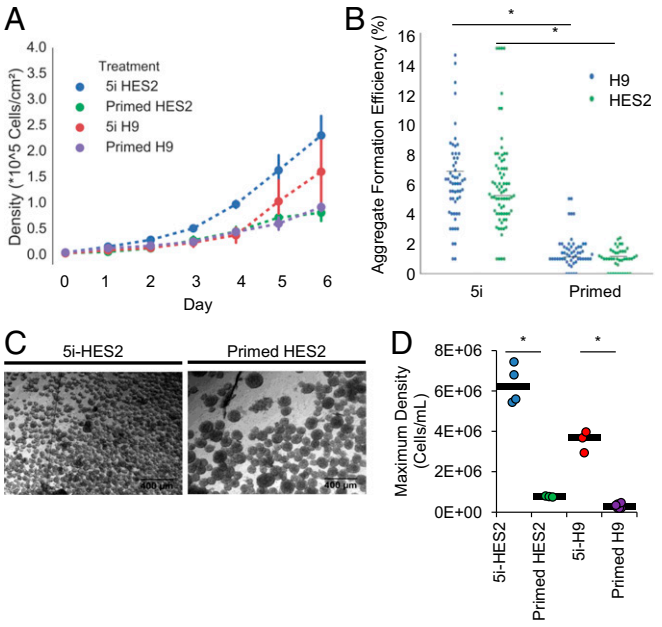

Fig. 2. Characterizing bioprocess parameters responsible for enhanced manufacturability. (*A*) Adherent growth curves for primed and 5i-hPSC (HES2 and H9 cell lines) on fibroblast feeder layers. Error bars represent the SD. (*B*) 5i-hPSC have a significantly higher single-cell colony formation efficiency in suspension than primed cells in both HES2 and H9 cell lines ($P < 0.05$, Kruskal–Wallis test, $n = 4$). (*C*) In an orbital shaker suspension bioreactor after 72 h of culture, 5i-HES2 form a larger number of smaller aggregates than primed HES2. (*D*) Maximum cell density reached by day 8 of culture in suspension. Cell densities reached in 5i conditions were significantly higher than in primed conditions ($P < 0.05$, Tukey's test, $n = 4$ 5i-HES2, $n = 3$ 5i-H9 and primed HES2).

Downloaded at Palestinian Territory, occupied on December 4, 2021
www.manaraa.com

8 h in suspension culture, 5i-H9 formed aggregates of varying sizes under both dynamic (orbital shaker) and static control conditions. Primed H9 formed small aggregates in the static control. However, in dynamic conditions, larger, irregular, and dark clumps formed (*SI Appendix*, Fig. S2*B*), suggesting the presence of dead cells and debris. After 72 h in suspension bioreactor culture, 5i-hPSC aggregate size appeared more homogeneous and smaller than primed hPSC aggregates (average diameters of 51 ± 18 and 113 ± 43 μm, respectively) (Fig. 2*C* and *SI Appendix*, Fig. S2*C*). These findings suggest a greater capacity for suspension aggregate growth of 5i-hPSC before aggregate size becomes growth limiting.

The suspension growth curves for primed hPSC and 5i-hPSC had varied lag-phase timing, growth rate, and maximum cell density (Fig. 2*D*). Cell densities peaked at days 5–6 for primed HES2, which was used as the baseline for further comparisons. 5i-HES2 and H9 density peaked at days 7 and 8 (*SI Appendix*, Fig. S2*D*). The peak 5i-HES2 density ($6.32 \pm 0.9 \times 10^6$ cells/mL) represented a 25-fold expansion and was nearly sixfold greater than that of primed HES2 at their peak density ($7.73 \pm 0.3 \times 10^5$ cells/mL). Similar growth curves were obtained for the 5i-H9 cell line, which reached a maximum cell density of $3.5 \pm 0.5 \times 10^6$ cells/mL Dramatically higher proliferation rates were observed in 5i-hPSC, as represented by their average doubling times in suspension: 29.0 ± 1.3 and 34.9 ± 1.9 h for 5i-HES2 and 5i-H9, respectively, and 49.2 ± 1.2 h for primed HES2.

Culture Optimization Enables Long-Term, High-Yield Maintenance of the Pluripotent State in Suspension. While high cell expansion in short-term 5i-hPSC bioreactor cultures can be achieved, we observed a gradual loss of the pluripotent phenotype (OCT4+/SOX2+) (Fig. 3*A*), in contrast to suspension expansion of primed hPSC (16). We examined various culture parameters to identify whether loss of pluripotency was due to endogenous interactions, missing feeder-layer interactions, or one of the components in 5i medium.

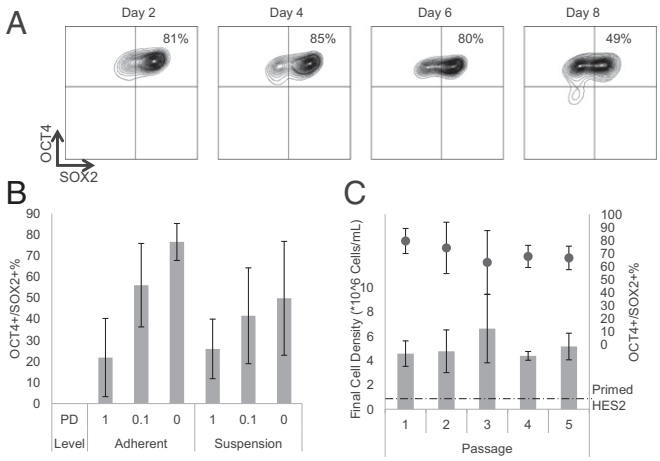

Fig. 3. A medium was identified that enables long-term maintenance of a pluripotent state in high-yield suspension culture. (*A*) Loss of the OCT4/SOX2 positive pluripotent phenotype is observed over time in 5i-hPSC suspension cultures. (*B*) Adding the PD inhibitor to feeder-free 5i-hPSC results in decreases in the OCT4/SOX2 phenotype in both adherent and suspension conditions in a 24-well format. Error bars represent the SD. (*C*) Culturing HES2 in 5i medium without the PD inhibitor (4i) for five passages resulted in maintenance of the pluripotent phenotype and cell densities in the range of 5×10^6 cells/mL, higher than cell densities achieved for primed HES2 (dashed line) that averaged $6.7 \pm 0.2 \times 10^5$ cells/mL. Error bars represent the SD. Numbers of replicates for each of the five passages shown are (n = 12, 7, 7, 6, 6) for final cell density and (n = 14, 9, 4, 3, 3) for OCT4/SOX2%.

In short-term bioreactor studies, we observed high pluripotent phenotype at the peak cell densities reached in primed hPSC cultures, but not at the peak densities achieved in 5i-hPSC cultures (*SI Appendix*, Fig. S3*A*). To develop a bioreactor protocol to maintain pluripotency of 5i-hPSCs, we first explored a strategy in which cells were passaged at the last day on which >80% of cells expressed a pluripotent phenotype (day 6), with the hypothesis that large aggregate size inhibits pluripotency through media limitations beyond this time point. However, we were unable to maintain a pluripotent phenotype in 5i-hPSC cultured in suspension beyond two passages with this strategy (*SI Appendix*, Fig. S3*B*). We next investigated whether optimization of dissociation timing may improve pluripotency by decreasing maximum aggregate size or increasing nutrient level per cell in culture, as has been recently suggested (30). On days 4, 5, 6, and 7 of 5i-hPSC suspension culture, the aggregates were either passaged to reduce aggregate size or diluted 1:10 in fresh medium to reduce the bulk cell density (see schematic in *SI Appendix*, Fig. S3*C*). However, after 4–7 d in both the dissociation experiment and the dilution experiment, no condition was able to maintain the pluripotent phenotype (*SI Appendix*, Fig. S3*D*). Since 5i medium maintains 5i-hPSC pluripotency in adherent feeder-based conditions, we speculated that the loss of the pluripotent phenotype was due to either the transition from adherent to suspension culture or to the loss of a specific interaction with the feeder layer.

To test our hypothesis, we designed a 96-well-plate platform to screen the effects of medium components on 5i-hPSC pluripotency in suspension and in feeder-free adherent cultures (*SI Appendix*, Fig. S3*C*). To separate the effects on pluripotency of adhesion from feeder-layer supportive factors, cells were cultured on a Geltrex-coated surface. On Geltrex, 5i-hPSC were still unable to propagate while maintaining a pluripotent phenotype (Fig. 3*B*, adherent "1PD" condition), suggesting that adhesion alone does not maintain pluripotency in the 5i medium. Next, we confirmed that suspension culture (low-adhesion coating) in the 96-well plate accurately replicated the kinetics of pluripotency loss (*SI Appendix*, Fig. S3*D*) in bioreactor culture, thereby providing a reliable platform to screen for critical suspension culture medium components. We performed a screen evaluating each of the components in 5i medium by either removing, doubling, or halving the concentration of each component. We observed improved feeder-free adherent maintenance of pluripotency upon removal of the ERK1/2 inhibitor (PD) from the 5i medium formulation (*SI Appendix*, Fig. S3*E*). We validated this finding in a dose–response experiment to determine the effect of PD concentration on pluripotent phenotype in both feeder-free adherent and suspension conditions (Fig. 3*B*). PD level was negatively correlated to pluripotent phenotype by linear regression (*SI Appendix*, Table S1). We next tested a number of molecules recently reported to further stabilize the naive pluripotent state to determine whether they enabled hPSC maintenance under feeder-free conditions in the presence of PD. Neither the SRC inhibitor CGP (23) nor YAP/TAZ activator LPA (25) supported the maintenance of the pluripotent phenotype in the presence of PD in suspension (*SI Appendix*, Fig. S4*A*). Interestingly, PD inhibits pluripotency in suspension, yet primed hPSC converted to an alternative state in the absence of PD (using the four-inhibitor formulation) did not have enhanced suspension expansion properties. In suspension, they show poor aggregation with a dark, heterogeneous aggregate morphology typical of primed hPSC (*SI Appendix*, Fig. S4*B*). These findings demonstrate the critical role that the ERK pathway plays in this cell-state conversion and in maintenance of pluripotency in suspension.

Next, hPSC cultured in adherent 5i conditions were treated without PD in a 4i formulation in orbital shaker suspension. "4i-hPSC " were cultured in suspension for five passages, achieving an average cell density of $5.2 \pm 1.1 \times 10^6$ cells/mL at passage 5 while maintaining a 67 ± 9% pluripotent phenotype (Fig. 3*C*).

Downloaded at Palestinian Territory, occupied on December 4, 2021
www.manaraa.com

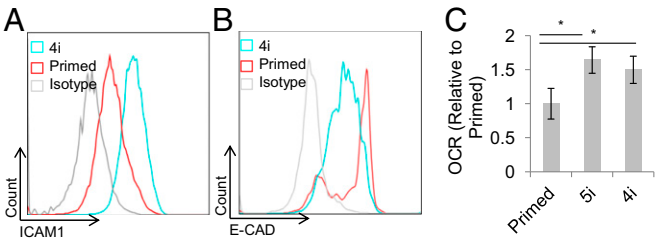

Fig. 4. Differential ICAM1 and E-CAD expression and oxygen consumption rate (OCR). (*A*) ICAM1 expression is elevated in 4i relative to primed HES2. (*B*) Primed E-CAD expression is bimodal, with a tight distribution of the high population. 4i expression is more widely distributed. (*C*) Relative OCRs of 4i and 5i-HES2 and primed HES2, as measured by the MitoXpress Xtra OCR assay. OCR is normalized to primed. * indicates $P < 0.05$ by *t* test. Error bars represent SD.

These results represent a 25 ± 5.5-fold cell expansion in 6 d that is 5.7 ± 0.2-fold greater than that achieved using primed HES2 in the same time period. hPSC cultured in 5i adherent culture for five passages and 4i suspension culture for three passages do not display karyotypic abnormalities (*SI Appendix*, Fig. S5*A*) and are able to differentiate into cells of all three germ layers (*SI Appendix*, Fig. S5*B*). To test the robustness of our 4i-hPSC system, we carried out an expansion using the H9 cell line, which in our hands is unable to expand in NutriStem medium and expands only moderately in conventional serum-replacement HES medium (~1.5-fold expansion after one passage) (*SI Appendix*, Fig. S6*A*). In suspension, 4i-H9 expanded nearly ninefold in 6 d while maintaining nearly 80% pluripotent marker expression (*SI Appendix*, Fig. S6*B*). These results show promise for the use of the 4i-hPSC culture system to enable suspension bioprocessing of hPSC lines that are not readily maintained in suspension. Suspension expansion of two additional lines, WIBR3 hESC and C1.15 hiPSC (*SI Appendix*, Fig. S6*C*), in 4i conditions led to significantly enhanced fold expansion (19.0 ± 2.0- and 21.5 ± 2.5-fold expansion, respectively) relative to primed hPSC, demonstrating that this technique is applicable to other hPSC lines including induced (i) PSC. Identifying the sources of variability in suspension performance between cell lines will guide the application of cell-state conversion strategies to improve suspension manufacturing.

Distinct Adhesion-Related Gene Expression and Medium Utilization in Suspension in 4i-hPSC. We hypothesized that the enhanced suspension properties of 4i-hPSC, including single-cell survival and aggregate formation, may be due to reduced expression of adhesion-related genes, which lowers the cells' dependence on adhesion for survival and maintenance of pluripotency. To identify whether adhesion-related genes are differentially expressed between 4i-hPSC and primed hPSC, we analyzed a panel of adhesion-related genes by qPCR. Notably, several genes related to the extracellular matrix as well as a variety of integrin molecules were observed to have differential expression between 4i-hPSC and primed conditions ($P > 0.05$, Tukey's test) (*SI Appendix*, Fig. S7). As qPCR results alone cannot predict gene expression, we validated select pluripotency-associated differentially expressed genes by flow cytometry. We identified elevated expression of adhesion-related gene ICAM1 in 4i-hPSC relative to primed hPSC (Fig. 4*A*). Primed E-CAD expression was observed to be bimodal, with a tight E-CAD^{high} population. hPSC treated with 4i expressed a wider, unimodal E-CAD distribution between the primed E-CAD^{low} and E-CAD^{high} populations (Fig. 4*B*). Additional characterization of the interaction between cell state and culture conditions for these and other correlated markers could supplement characterization of causal factors in supporting this altered pluripotent state (29).

Next, we compared the metabolic demand and activity of 4i-hPSC to primed hPSC by comparing oxygen consumption rate (OCR) (Fig. 4*C*) and metabolite levels in the medium over 6 d of suspension culture. Glucose levels dropped from their initial level in all conditions, reaching a steady level by day 2 in primed conditions but not in 4i-hPSC. While 4i-hPSC continued to grow to higher densities even at lower glucose levels, the steady glucose levels in primed hPSC suggested that primed cells may require higher glucose levels for growth. Indeed, glucose uptake per cell was much lower for 4i-hPSC than primed cells, although differences in specific uptake between primed media suggest that nutrient availability may contribute to these trends. In contrast to primed conditions, in 4i culture, glutamine and glutamate dropped after day 3 at the same rate as cell expansion (*SI Appendix*, Fig. S8). Lactate production varied independently of cell state, while ammonium levels were highest in 4i-hPSC cultures (*SI Appendix*, Fig. S8). These metabolite trends lead to an elevated oxygen consumption rate of 4i-hPSC (and 5i-hPSC) relative to primed (Fig. 4*C*). These altered-state hPSC therefore display a metabolic usage distinct from that of primed hPSC that appears independent of base nutrient differences between the conditions.

Directed Differentiation of 4i-hPSC to Pancreatic Progenitors Does Not Require Repriming. We next tested the capacity for alternative-state hPSC to differentiate to pancreatic progenitors, a cell type of significant clinical interest. Directed differentiation to pancreatic progenitors from hPSC is achieved by the staged addition of molecules intended to mimic development (31) (*SI Appendix*, Fig. S9*A*). Our initial attempts to differentiate adherent 5i-hPSC (Fig. 5*A*) and recent reports on differentiation of

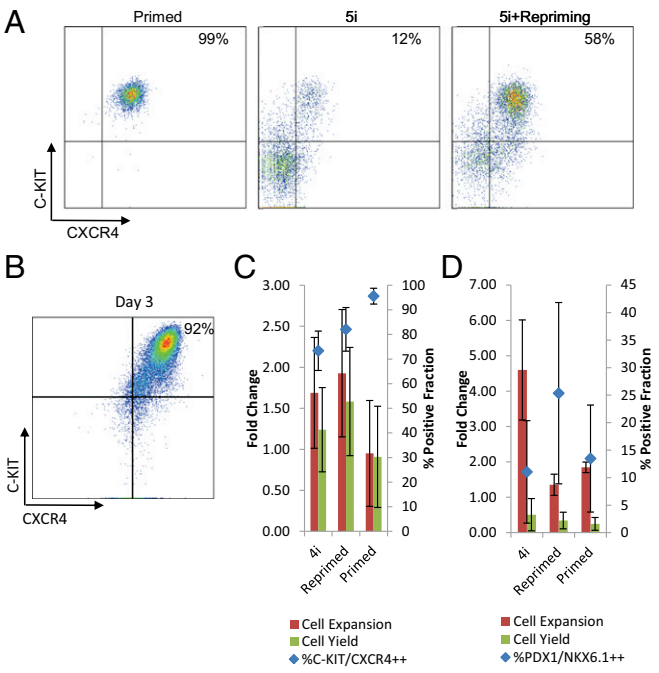

Fig. 5. 4i-hPSC can be directed to differentiate to pancreatic progenitors without repriming. (*A*) Differentiation of primed hPSC results in a high (>95%) percentage of definitive endoderm marked by c-kit/cxcr4 expression after 3 d in an adherent differentiation. 12% of differentiated 5i-hPSC express this phenotype at day 3 of differentiation, whereas 5i-hPSC reprimed in serum replacement medium expressed this phenotype at 58% purity (representative experiment shown). (*B*) In suspension-optimized conditions, 4i-hPSC differentiate to a definitive endoderm phenotype at levels reaching 95% after 3 d. 4i-hPSC and primed hPSC can differentiate to (*C*) definitive endoderm and (*D*) pancreatic progenitors with comparable cell yields and purities. No significant difference was observed at day 3 in fold expansion and yield. Primed hPSC had significantly higher purity ($P < 0.005$, Tukey's test). At day 12, no significant difference was observed in purity or yield, although 4i-hPSC had significantly higher fold expansion ($P < 0.01$, Tukey's test). Error bars in this figure represent SD.

Downloaded at Palestinian Territory, occupied on December 4, 2021
www.manaraa.com

naive hPSC (32, 33) suggested that current differentiation protocols for primed hPSC result in low purity or cell yield when applied to 5i-hPSC. We hypothesized that 5i-hPSC could be differentiated to clinically relevant lineages by culturing 5i-hPSC in primed hPSC conditions before differentiation. Indeed, we found that "repriming" adherent 5i-hPSC for 1 d before differentiation increased the fraction of definitive endoderm cells at day 3 of differentiation (Fig. 5*A*).

We next sought to identify conditions that would enable suspension differentiation. While a 2-d repriming strategy enabled suspension differentiation of 5i-hPSC, we found that our 4i-hPSC formulation could be efficiently differentiated toward pancreatic progenitors without a repriming step. Both 2-d repriming with Nutristem feeder-free medium as well as 4i-hPSC conditions resulted in high-purity (>90%) definitive C-KIT/CXCR4 endoderm phenotype after 3 d (Fig. 5 *B* and *C*) with the capacity to generate PDX1/NKX6.1 endocrine pancreatic cells after 12 d (Fig. 5*D*). Comparing outcomes from these strategies did not result in statistically significant differences in purity, expansion, or yield after 3 d of definitive endoderm differentiation, although 4i-hPSC had a significantly greater number of cells after 12 d of differentiation relative to reprimed 5i-hPSC ($P < 0.01$, Tukey's test), with no significant difference in purity. 4i-hPSC are thus capable of pancreatic progenitor differentiation.

Discussion

Our study demonstrates that culture conditions may be manipulated to generate pluripotent states that can overcome bottlenecks in manufacturing of hPSC and their differentiated derivatives. Improved growth and maintenance of 4i-hPSC in suspension is mediated by increased shear tolerance and altered aggregation properties that promote efficient suspension colony formation leading to faster growth rates and higher achievable maximum cell densities. 4i-hPSC thus represents a more manufacturable pluripotent state characterized by the formation of a larger number of smaller aggregates which grow faster and are less susceptible to bioreactor shear-induced cell death over multiple passages in suspension, while retaining directed differentiation capability. The manufacturability of 4i-hPSC can be compared to published hPSC suspension expansion in *SI Appendix*, Fig. S9*B*.

Metabolic analysis of suspension 4i-hPSC suggests bivalent glycolytic and oxidative metabolism. 4i-hPSC had lower glucose consumption and lactate secretion per cell than primed hPSC despite their faster growth rates, representative of the more efficient energy usage characteristic of oxidative metabolism (34). Interestingly, while glucose levels decline steadily from the outset, glutamine levels decline (and ammonium levels rise) most notably after day 4, suggesting preferential utilization of glucose in 4i-hPSC. These observations are consistent with recent reports that the pathways for bivalent metabolism are present in the naive state (22) but that glycolytic metabolism is preferred (35). Ultimately, however, metabolic pathway usage is dependent on nutrient availability (36), as is evident both by the shift to glutamine usage when glucose concentration is reduced and by the distinct metabolic profiles observed between the two primed medium compositions used (*SI Appendix*, Fig. S8). While this metabolic shift appears to begin at day 4 of culture, cells can continue to grow and maintain pluripotency for at least two more days of culture (Fig. 3*E*). This finding suggests that significant opportunities exist for improving suspension yields through medium optimization to promote pathways that drive expansion without loss of pluripotency. Strategies could include enriched medium for high-density culture and modified medium exchange methods or rates.

The hypothesis that cellular conversion to alternative pluripotent states could overcome manufacturing challenges guided the development and optimization of the 4i-hPSC suspension system. The extent to which these improvements can be attributed to modulation of cell state depends on how cell state is defined. To date, many efforts to generate a naive hPSC state are deemed successful based solely on similar gene expression profiles to naive mouse PSC. In a manufacturing context defining cell state by gene expression and purported similarity to a developmental cell state in mice is less relevant than functional definitions of alternative cell states. In this regard, the 4i-hPSC culture has clearly enabled an alternative pluripotent state that is highly amenable to high-yield suspension culture, both in bioprocess-related cellular properties and in energy-efficient metabolic pathway usage.

We hypothesize that the more robust suspension aggregation properties of 4i-hPSC (Fig. 2 *B* and *C*) could have been caused by altered adhesion-related gene expression between the cell states (Fig. 4 *A* and *B*). The role of ICAM1 in pluripotency is not well described. We observed elevated expression of ICAM1 in 4i-hPSC (Fig. 4*A*). While implicated in reprogramming to pluripotency (29), it remains to be seen if ICAM1 is causative of aggregation properties observed in 4i-hPSC or if it arises as a result of altered cell-adhesion patterns associated with this cell state. Primed E-CAD expression has been observed by Xu et al. (37) to be bimodal. They suggested that E-CAD^{low} cells had poor suspension survival because of a lack of E-CAD–mediated cell–cell adhesion, whereas E-CAD^{high} cells have greater potential to survive post-dissociation. They did not observe this dependence in mouse ESC or hESC treated with ERK1/2 and p38 inhibitors due to different regulation of E-CAD, leading to increased stability. Comparing primed and 4i expression of E-CAD in our study further supports different mechanisms of suspension survival between conditions (Fig. 4*B*). Tightly controlled, high expression of primed E-CAD suggests this protein may be important for proliferation and survival of primed hPSC. In contrast, we hypothesize that the broad spread of E-CAD in 4i-hPSC suggests that cell survival may be less linked to E-CAD, since high expression is not necessary. Indeed, 4i treatment reduced suspension passaging-related aggregation challenges and cell death (Fig. 2 *B* and *C*).

Not surprisingly, analyzing published reports of suspension expansion of mouse and hPSC (*SI Appendix*, Fig. S9*B*) illustrates that 4i-hPSC are distinct from traditional hPSC cultures in suspension expansion yield, intensification (i.e., cell density), and growth rates, and are more in line with mouse PSC. Encouragingly, this relatively unoptimized bioprocess could be further enhanced by incorporating perfusion feeding schemes, medium optimization, and additional molecules to further enhance the alternative cell state. Media optimization around endogenous and exogenous factors and aggregation control could prove instrumental in reducing variability in long-term suspension expansion of 4i-hPSC.

Interestingly, ERK inhibition, which blocks FGF4 differentiation signals and establishes the naive state (28), led to a loss of the pluripotent phenotype in suspension but not adherent 5i-hPSC on feeders. Removal of ERK inhibition maintained a pluripotent phenotype in suspension without diminishing the cells' preferential suspension bioprocessing capabilities. ERK appears to cause an exit from pluripotency through a mechanism unique to the suspension environment. Adhesion and growth factor signals are thought to be integrated by RAC-facilitated formation of two distinct signaling complexes: ERK-MEK1 in adherent culture, and ERK-MEK2 in suspension culture (38). We hypothesize that the extended culture in adherent conditions in the presence of ERK_i converted cells to an alternative, high-suspension-yield attractor state that is not exited upon removal of ERK_i in suspension culture. The use of transient cues to acquire an attractor state has been well established in the PSC field largely through the transient overexpression of factors inducing reprogramming of somatic cells to pluripotency (39). Further study of these mechanisms may determine whether suspension culture in the presence of PD is possible or beneficial.

Combining directed differentiation protocols with the high-yield 4i-hPSC expansion system could form the basis for efficient expansion-differentiation strategies for manufacturing various

ENGINEERING
APPLIED BIOLOGICAL SCIENCES
Downloaded at Palestinian Territory, occupied on December 4, 2021
www.manaraa.com

therapeutic cell types. While we observed that ERK inhibition hampered directed differentiation of 5i-hPSC, transferring to 4i or primed medium for a short period before initiating an established differentiation protocol enabled this differentiation. The outcomes using the 4i-hPSC bioprocess exceed those observed in any hPSC suspension expansion system, and are within the range of high-yield mouse PSC systems (*SI Appendix*, Fig. S9*B*). Importantly, 4i-hPSCs could enable scalable, high-yield production of pancreatic progenitors, which are a key intermediate cell in generating islet cells for transplantation therapies targeting type 1 diabetes. Our results highlight cell-state conversion as a key component to overcome manufacturing challenges in novel cell therapy bioprocessing strategies (40).

Methods and Materials

Primed hPSC were cultured on Geltrex-coated plates in Nutristem hESC Culture Medium. Where noted, hPSC were cultured on irradiated mouse embryonic fibroblast feeders in serum replacement medium (DMEM/F12, knockout serum replacement, Glutamax, nonessential amino acids, penicillin-streptomycin, and FGF2). To convert hPSC to an alternative pluripotent state, primed hPSC cultured on feeder layers were treated as described previously with modifications recommended by Hanna (27). In brief, base medium contained DMEM/F12, knockout serum replacement, Glutamax, nonessential amino acids, penicillin-streptomycin, Albumax 2, N2 supplement, insulin, and ascorbic acid. This medium was supplemented with LIF, TGFβ1, FGF2, CHIR99021, SP600125, BIRB796, Gö6983, and PD0325901 where noted. Dynamic suspension cultures were carried out in six-well plates (coated overnight with 5% Pluronic F-68) on an orbital shaker and bioreactor runs were performed using the Micro-24 bioreactor system (Pall Corporation). hPSC were seeded at a density of 2×10^5 cells/mL in either NS medium, SR medium, or our treatment formulation supplemented with Y-27632. Half of the medium was exchanged daily starting from day 2. Treated and untreated cells were differentiated toward endoderm, mesoderm, and ectoderm using staged differentiation protocols.

RNA was extracted for qPCR using the RNeasy Mini Kit, and reverse transcribed using the SuperScript II kit according to manufacturer's instructions. Analysis was performed using the delta-delta Ct method, normalizing to GAPDH and primed expression level. Metabolite usage was determined from media supernatants, and oxygen consumption rate was measured using the MitoXpress Xtra oxygen tracker kit. G-Band karyotyping was performed by WiCell.

Parametric tests were used to analyze qPCR, doubling time, and maximum density experiments, with the Student's *t* test used for two treatment experiments and Tukey's test used for experiments with three or more treatments. A nonparametric test (Kruskal–Wallis) was used for colony formation experiments. * signifies $P < 0.05$ unless otherwise noted. The linear regression model was developed in Excel.

Details are found in *SI Appendix, Supporting Methods*.

ACKNOWLEDGMENTS. We thank P. Luecker for guidance with cardiac differentiation experiments. Y.Y.L. is supported by a Natural Science and Engineering Research Council Alexander Graham Bell Canada Graduate Scholarship, C.W. is supported by a Canadian Institute for Health Research Doctoral Research Award, and P.W.Z. is supported as the Canada Research Chair in Stem Cell Bioengineering.

1. Kirouac DC, Zandstra PW (2008) The systematic production of cells for cell therapies. *Cell Stem Cell* 3:369–381.
2. Lipsitz YY, Timmins NE, Zandstra PW (2016) Quality cell therapy manufacturing by design. *Nat Biotechnol* 34:393–400.
3. Baptista RP, Fluri DA, Zandstra PW (2013) High density continuous production of murine pluripotent cells in an acoustic perfused bioreactor at different oxygen concentrations. *Biotechnol Bioeng* 110:648–655.
4. Fernandes-Platzgummer A, Diogo MM, Baptista RP, da Silva CL, Cabral JM (2011) Scale-up of mouse embryonic stem cell expansion in stirred bioreactors. *Biotechnol Prog* 27:1421–1432.
5. Cormier JT, zur Nieden NI, Rancourt DE, Kallos MS (2006) Expansion of undifferentiated murine embryonic stem cells as aggregates in suspension culture bioreactors. *Tissue Eng* 12:3233–3245.
6. Shafa M, et al. (2012) Expansion and long-term maintenance of induced pluripotent stem cells in stirred suspension bioreactors. *J Tissue Eng Regen Med* 6:462–472.
7. Kehoe DE, Lock LT, Parikh A, Tzanakakis ES (2008) Propagation of embryonic stem cells in stirred suspension without serum. *Biotechnol Prog* 24:1342–1352.
8. zur Nieden NI, Cormier JT, Rancourt DE, Kallos MS (2007) Embryonic stem cells remain highly pluripotent following long term expansion as aggregates in suspension bioreactors. *J Biotechnol* 129:421–432.
9. Fok EYL, Zandstra PW (2005) Shear-controlled single-step mouse embryonic stem cell expansion and embryoid body-based differentiation. *Stem Cells* 23:1333–1342.
10. Abranches E, Bekman E, Henrique D, Cabral JMS (2007) Expansion of mouse embryonic stem cells on microcarriers. *Biotechnol Bioeng* 96:1211–1221.
11. Fernandes AM, et al. (2007) Mouse embryonic stem cell expansion in a microcarrier-based stirred culture system. *J Biotechnol* 132:227–236.
12. Amit M, et al. (2011) Dynamic suspension culture for scalable expansion of undifferentiated human pluripotent stem cells. *Nat Protoc* 6:572–579.
13. Chen VC, et al. (2012) Scalable GMP compliant suspension culture system for human ES cells. *Stem Cell Res (Amst)* 8:388–402.
14. Zweigerdt R, Olmer R, Singh H, Haverich A, Martin U (2011) Scalable expansion of human pluripotent stem cells in suspension culture. *Nat Protoc* 6:689–700.
15. Olmer R, et al. (2012) Suspension culture of human pluripotent stem cells in controlled, stirred bioreactors. *Tissue Eng Part C Methods* 18:772–784.
16. Lipsitz YY, Zandstra PW (2015) Human pluripotent stem cell process parameter optimization in a small scale suspension bioreactor. *BMC Proc* 9:O10.
17. Kehoe DE, Jing D, Lock LT, Tzanakakis ES (2010) Scalable stirred-suspension bioreactor culture of human pluripotent stem cells. *Tissue Eng Part A* 16:405–421.
18. Rossant J, Tam PPL (2017) New insights into early human development: Lessons for stem cell derivation and differentiation. *Cell Stem Cell* 20:18–28.
19. Brons IGM, et al. (2007) Derivation of pluripotent epiblast stem cells from mammalian embryos. *Nature* 448:191–195.
20. Tesar PJ, et al. (2007) New cell lines from mouse epiblast share defining features with human embryonic stem cells. *Nature* 448:196–199.
21. Chan Y-S, et al. (2013) Induction of a human pluripotent state with distinct regulatory circuitry that resembles preimplantation epiblast. *Cell Stem Cell* 13:663–675.
22. Takashima Y, et al. (2014) Resetting transcription factor control circuitry toward ground-state pluripotency in human. *Cell* 158:1254–1269.
23. Theunissen TW, et al. (2014) Systematic identification of culture conditions for induction and maintenance of naive human pluripotency. *Cell Stem Cell* 15:471–487, and erratum (2014) 15:524–526.
24. Ware CB, et al. (2014) Derivation of naïve human embryonic stem cells. *Proc Natl Acad Sci USA* 111:4484–4489.
25. Qin H, et al. (2016) YAP induces human naive pluripotency. *Cell Rep* 14:2301–2312.
26. Zimmerlin L, et al. (2016) Tankyrase inhibition promotes a stable human naïve pluripotent state with improved functionality. *Development* 143:4368–4380.
27. Gafni O, et al. (2013) Derivation of novel human ground state naive pluripotent stem cells. *Nature* 504:282–286.
28. Ying Q-L, et al. (2008) The ground state of embryonic stem cell self-renewal. *Nature* 453:519–523.
29. Shakiba N, et al. (2015) CD24 tracks divergent pluripotent states in mouse and human cells. *Nat Commun* 6:7329.
30. Kropp C, et al. (2016) Impact of feeding strategies on the scalable expansion of human pluripotent stem cells in single-use stirred tank bioreactors. *Stem Cells Transl Med* 5:1289–1301.
31. Nostro MC, et al. (2015) Efficient generation of NKX6-1+ pancreatic progenitors from multiple human pluripotent stem cell lines. *Stem Cell Reports* 4:591–604.
32. Geula S, et al. (2015) Stem cells. m6A mRNA methylation facilitates resolution of naïve pluripotency toward differentiation. *Science* 347:1002–1006.
33. Irie N, et al. (2015) SOX17 is a critical specifier of human primordial germ cell fate. *Cell* 160:253–268.
34. Carbognin E, Betto RM, Soriano ME, Smith AG, Martello G (2016) Stat3 promotes mitochondrial transcription and oxidative respiration during maintenance and induction of naive pluripotency. *EMBO J* 35:618–634.
35. Gu W, et al. (2016) Glycolytic metabolism plays a functional role in regulating human pluripotent stem cell state. *Cell Stem Cell* 19:476–490.
36. Zhang H, et al. (2016) Distinct metabolic states can support self-renewal and lipogenesis in human pluripotent stem cells under different culture conditions. *Cell Rep* 16:1536–1547.
37. Xu Y, et al. (2010) Revealing a core signaling regulatory mechanism for pluripotent stem cell survival and self-renewal by small molecules. *Proc Natl Acad Sci USA* 107:8129–8134.
38. Eblen ST, Slack JK, Weber MJ, Catling AD (2002) Rac-PAK signaling stimulates extracellular signal-regulated kinase (ERK) activation by regulating formation of MEK1-ERK complexes. *Mol Cell Biol* 22:6023–6033.
39. Takahashi K, et al. (2007) Induction of pluripotent stem cells from adult human fibroblasts by defined factors. *Cell* 131:861–872.
40. Lipsitz YY, Bedford P, Davies AH, Timmins NE, Zandstra PW (2017) Achieving efficient manufacturing and quality assurance through synthetic cell therapy design. *Cell Stem Cell* 20:13–17.

Downloaded at Palestinian Territory, occupied on December 4, 2021
www.manaraa.com